

## Evaluation of rotating shadowband radiometer measurements in desert conditions

Dunia Bachour<sup>1</sup> and Daniel Perez-Astudillo<sup>1</sup>

<sup>1</sup> Qatar Environment and Energy Research Institute, HBKU, Qatar Foundation, Doha (Qatar)

### Abstract

Ground measurement of solar radiation is the most accurate way to evaluate and quantify the available solar resources at any specific site. This is particularly important for solar energy projects. The acquisition of high quality solar radiation data requires the installation of a solar radiation monitoring station with thermoelectric type of sensors such as pyranometers and pyrhelimeter, mounted on a sun-tracker system. This type of station allows the collection of reliable solar radiation data, but it is costly and requires continuous maintenance. An alternative method for on-site measurements of solar radiation is the use of a rotating shadow band irradiometer (RSI) based on a photodiode sensor. The system is less expensive and requires less frequent maintenance; however, the collected data are less accurate. A study of the data measured by an RSI operating in desert conditions is presented here; This RSI has been calibrated and corrections have been applied by the manufacturer, but not for the local conditions at the site of this study. The results show the estimated uncertainties of solar components derived by RSI, when compared to the ones acquired by the thermopile-based sensors; the relative root mean square errors for GHI are less than 3 % and they are larger for the diffuse and direct components. The largest deviations are found for the direct component, which is computed by the RSI from the global and diffuse components, and not measured.

Keywords: solar resource, ground measurements, RSI,  $G_b$ ,  $G$ ,  $G_d$ .

---

### 1. Introduction

The assessment of solar resources requires determining three components of the incoming sunlight: direct normal irradiance ( $G_b$ ), global horizontal irradiance ( $G$ ) and diffuse horizontal irradiance ( $G_d$ ). It is best to measure each component with a separate sensor of known uncertainty, ideally with thermoelectric radiometers, which provide the highest-quality measurements. However, these sensors have high prices and the measurement of  $G_b$  and  $G_d$  requires the use of a sun tracker, further increasing costs, complexity and maintenance requirements. A common alternative are rotating shadowband radiometers (RSRs), which use only one sensor (a photodiode) to measure  $G$  and, with the help of a shading band that rotates regularly,  $G_d$ ; from these two,  $G_b$  is calculated using SZA, the solar zenith angle, through

$$G = G_b \cdot \cos(\text{SZA}) + G_d \quad (\text{Eq.1})$$

Operating an RSI instead of a sun tracker-based solar monitoring station has several advantages. First of all, only one instrument is required to obtain the three solar radiation components. Among other advantages, RSIs have lower cost, are less sensitive to sensor soiling (Pape et al., 2009), and require less maintenance. RSIs use silicon detectors that have faster response times compared to thermopile detectors; on the other hand, they have a narrow spectral response, which provides systematic deviations of their response, resulting in lower accuracies in determining broadband solar radiation (Wilbert et al., 2015). RSI accuracy also depends on the operation conditions since the silicon photodiode detectors are temperature dependent, so the RSI suitability should be studied depending on the intended use, and correction functions should be applied to correct for the systematic deviations. The study presented here compares solar radiation measured by RSI to solar radiation measured by thermopile-based sensors under desert conditions.

## 2. Methodology

The analyzed data in this study were collected during one year, from November 2013 until October 2014, at the Qatar Energy and Environment Research Institute (QEERI), located in Education City, Doha, Qatar (25.325°N, 51.433°E). Measurements of solar irradiances were taken at 1-minute resolution with a Kipp and Zonen thermoelectric sensor-based monitoring station. This high-quality station is equipped with two CMP11 pyranometers for global and diffuse measurements and one CHP1 pyrhelimeter for direct solar radiation measurements, with all sensors mounted on a Solys2 sun tracker. The thermoelectric sensor measurements, hereafter designed by KZ, are compared with the corresponding measurements taken at the same time and location with an RSR2 radiometer, from Irradiance, Inc., hereby called RSR and consisting of a Licor LI-200 silicon photodiode pyranometer and a band driven by a motor, which shades the sensor temporarily from the direct sunlight in order to make the diffuse measurement, and by using Eq.1 the direct normal irradiance is calculated.

All sensors (RSR and KZ) are factory calibrated by their respective manufacturer, following international standards. The data analyzed in this study are acquired by the abovementioned sensors operating within less than two years since their calibration date. According to the RSR2 ‘Certificate of Calibration’ document from the manufacturer (Irradiance), the calibration value is produced with “corrections for spectral, angle of incidence and temperature dependencies of the diffusers and silicon photodiode used in LI-CORs pyranometer sensors”. Correction functions are applied separately on the global and diffuse sensor responses in RSR2, and are described in Augustyn et al. (2004).

The two monitoring stations were maintained regularly (at least 4 times during the week) including cleaning and checking the alignment of all sensors, except in specific experimental periods in which soiling of RSR were studied and the RSR sensor was cleaned less often. The data of the soiling campaign are not included in the analysis here except for the monthly averages as will be explained later. In addition, only data of both instruments that passes the quality control tests described in Long and Dutton, (2002) were used.

Figure 1 shows the KZ station (left side) and the RSR2 (right side), installed in Education City.



Fig.1: Solar monitoring stations operating in Education City, Doha, Qatar.

For the comparison, scatter plots comparing the RSR data against the KZ data are studied, as well as the mean bias difference (MBD), root-mean-square-difference (RMSD) and their relative values rMBD and rRMSD were calculated.

$$MBD = \frac{1}{n} \sum_i (x_{RSR,i} - x_{KZ,i}) \quad (eq.2)$$

$$RMSD = \sqrt{\sum_i \frac{(x_{RSR,i} - x_{KZ,i})^2}{n}} \quad (\text{eq.3})$$

where  $i$  goes from 1 to  $n$ , and consists of all pairs of RSR and KZ data with the same timestamp, during daytime.  $x_{KZ,i}$  and  $x_{RSR,i}$  are the irradiance values ( $G_b$ ,  $G$ , and  $G_d$ ) from the KZ and RSR measurements, respectively. The relative values rMBD and rRMSD are computed by dividing MBD and RMSD by the corresponding averages of the KZ values. Possible dependencies of the errors on zenith angle and ambient temperature are also studied. In addition to the spectral dependency, these are expected to be the main factors affecting the RSR; the RSR sensor is covered by a light diffuser shaped as a disk, so light transmission might be affected at the edges of this disk; and since the sensor is basically a photovoltaic cell, its signal varies with temperature and, although corrections are applied, some might not be optimal. For a more complete analysis, the three 'components' are studied here, namely direct normal irradiance, global horizontal irradiance, and diffuse horizontal irradiance.

### 3. Results

Figure 2 shows samples of the relative bias of the 10-minute averages of the three components, through several weeks, calculated as the difference of the 10-min average of RSR and KZ data at the particular timestamp, divided by the KZ value at the same timestamp. In general, the errors for  $G$  are within 5 % (absolute value); they are higher for the diffuse component, and the largest errors occur for  $G_b$ . Larger deviations occur at high zenith angles (low sun elevations) for all components, from which each day can be distinguished in the plot. This is especially obvious for  $G_b$ , because RSR  $G_b$  is computed following equation 1, which requires the calculation of the cosine of the solar zenith angle, and any uncertainties in this calculation reflect in  $G_b$  calculated values (Vignola, 2006). The systematic overestimation observed in  $G_d$  measured by RSR may be due to an insufficient correction of the excess sky hidden by the shadowband applied to the diffuse component. Indeed, when the shading band rotates, apart from obscuring the sun it blocks a part of the sky; to correct for the excess obstruction, samples just before and after the solar disk is blocked are used in a correction based on the position of the maximum slope of an abrupt fall of the  $G$  signal (Irradiance, 2019; Wilbert et al., 2015). Due to larger solar disk observed in Qatar's conditions, the slope variation is slower, resulting in an overestimation of the correction added to  $G_d$ .

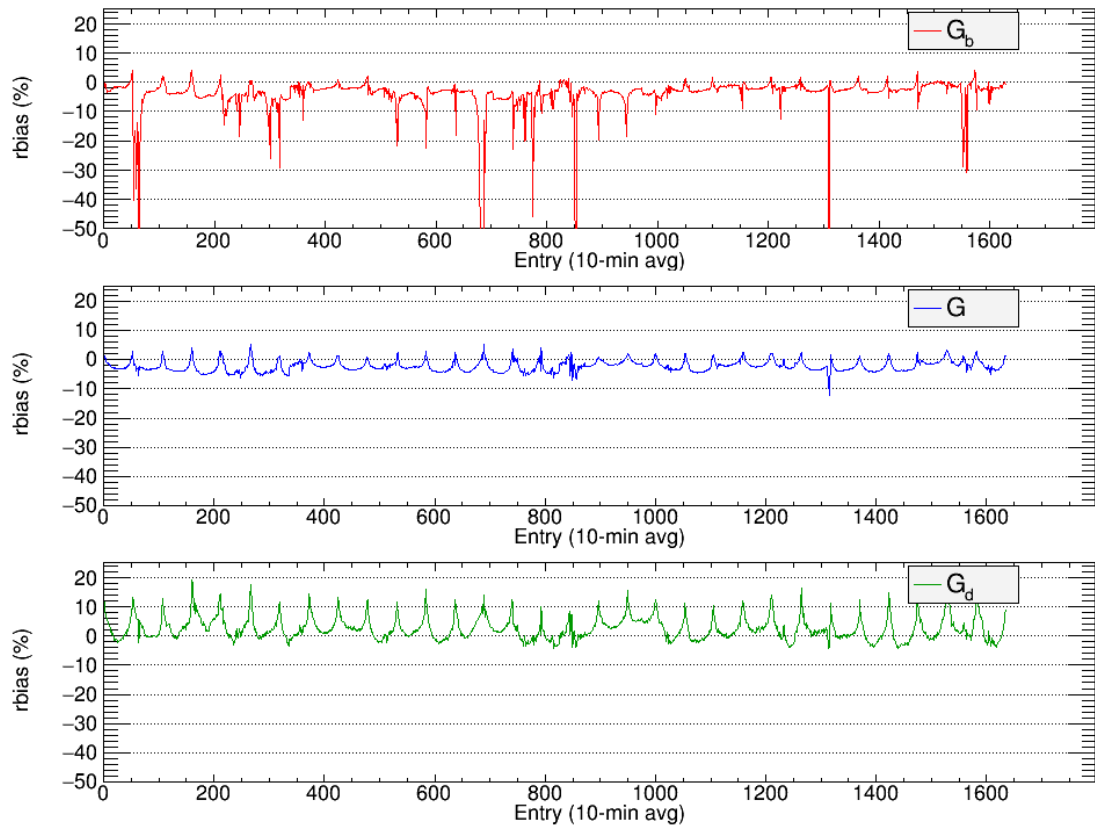


Fig.2: rMBD of RSR measurements w.r.t. thermoelectric ones, using 10-minute averages, over several weeks.

Figure 3 illustrates the one-to-one correlations of daytime measurements of RSR versus KZ for the three components, using one-minute averages, as measured by both stations.

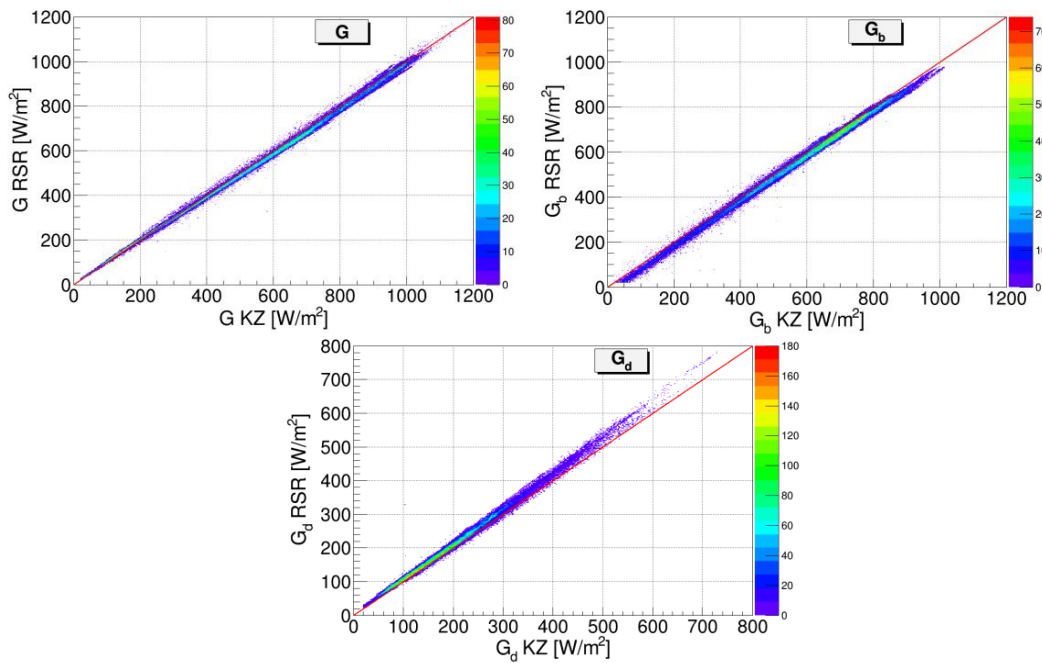


Fig.3: Comparison of  $G_b$ ,  $G$ , and  $G_d$  as measured by RSR and KZ during 1 year in Doha, Qatar.

It can be seen that in general  $G$  is well correlated with slight underestimation of RSR values compared to KZ

values.  $G_d$  shows however an overestimation, more noticeably at higher level of radiations.  $G_b$  follows the opposite behavior of  $G_d$ , and has in general larger errors since as mentioned before the uncertainties here are the combined effect of the inputs to its calculation. In table 1 are shown the values of the statistical comparisons for 1-min, 10-min and hourly averages, for daytime entries of zenith angle less than  $80^\circ$ . It is to be noted that the errors improve slightly with higher aggregations of the data, except for the diffuse component.

Tab. 1: Results of the comparison between RSR and KZ; MBD, and RMSD are in  $W/m^2$ ; rMBD and rRMSD are in %.

	MBD	rMBD	RMSD	rRMSD	Corr.
<b>1 min, SZA&lt;80°</b>					
$G_b$	-18.7117	-3.2464	22.324	3.87313	0.998251
$G$	-10.4841	-1.86237	15.4348	2.74182	0.999243
$G_d$	7.72834	3.91634	11.1016	5.62575	0.997537
<b>10 min, SZA&lt;80°</b>					
$G_b$	-18.5874	-3.27911	21.7395	3.83521	0.998571
$G$	-10.4808	-1.8617	15.1435	2.68995	0.999296
$G_d$	7.71858	3.91082	10.8954	5.52042	0.997703
<b>1 hour, SZA&lt;80°</b>					
$G_b$	-17.8074	-3.20848	21.3694	3.85027	0.998458
$G$	-9.75044	-1.7389	15.4058	2.74759	0.999135
$G_d$	7.91014	4.02086	10.8938	5.53572	0.997653

Considering higher temporal aggregations, figure 4 shows the monthly averages of  $G_b$ ,  $G$ , and  $G_d$  calculated from quality-controlled 1-min KZ and RSR data, without excluding the data from the experimental periods mentioned in section 2 in order to keep the representativeness of the monthly values. Differences can be seen when comparing the results month by month, however with almost the same trend throughout the year. The yearly relative biases calculated from the monthly average irradiance values, respectively for  $G_b$ ,  $G$  and  $G_d$  are: -6.215%, -3.684%, and 2.235%. The biases are more shifted towards negative when compared to the values in table 1, due to the decrease in the RSR signal because of the soiling.

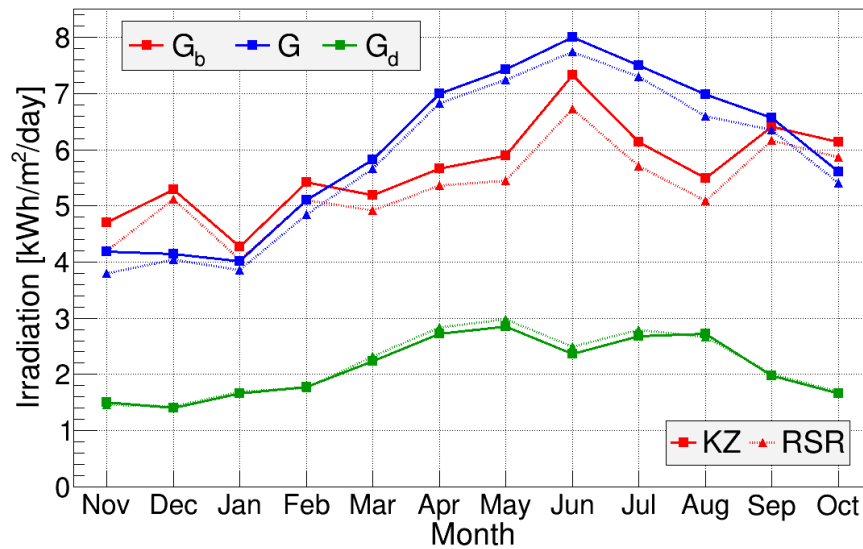


Fig.4: Monthly averages of  $G_b$ ,  $G$ , and  $G_d$  measured in Doha, Qatar.

Systematic deviations in the RSR measurements when compared to the thermopile-based sensors can also be

due to cosine response errors and to the temperature dependence as well (King et al., 1998; Vignola et al., 2017). Figures 5 and 6 show respectively the relative bias as a function of air temperature and zenith angle for the three components, calculated as the difference between the one-min value of RSR and KZ data at the particular timestamp, divided by the one-min KZ value at the same timestamp. In figure 5, there is no clear dependency on temperature. For the diffuse component, the dispersion of the relative biases seems slightly more widespread than for the global one with no clear temperature dependence either, but with mostly positive rMBD. As explained previously, this may be due to the method applied to the diffuse component derived by the RSR. Another correction, related to the spectral effect, takes part in the estimation of RSR  $G_d$  as explained in (Vignola et al., 2017). These two corrections may be insufficient and result in an overestimation of the RSR-measured diffuse irradiance in Qatar's conditions, where 'clear' skies (cloudless) are still highly loaded with aerosols, which affects the expected clear-sky spectrum. Similarly,  $G_b$  does not show any clear temperature dependency; however, the dispersion of rMBD is the largest since the errors in  $G$  and  $G_d$  are amplified in the RSR-calculated  $G_b$ , as discussed previously. A large part of  $G_b$  deviations are negative; the main cause is the overestimation seen in  $G_d$ .

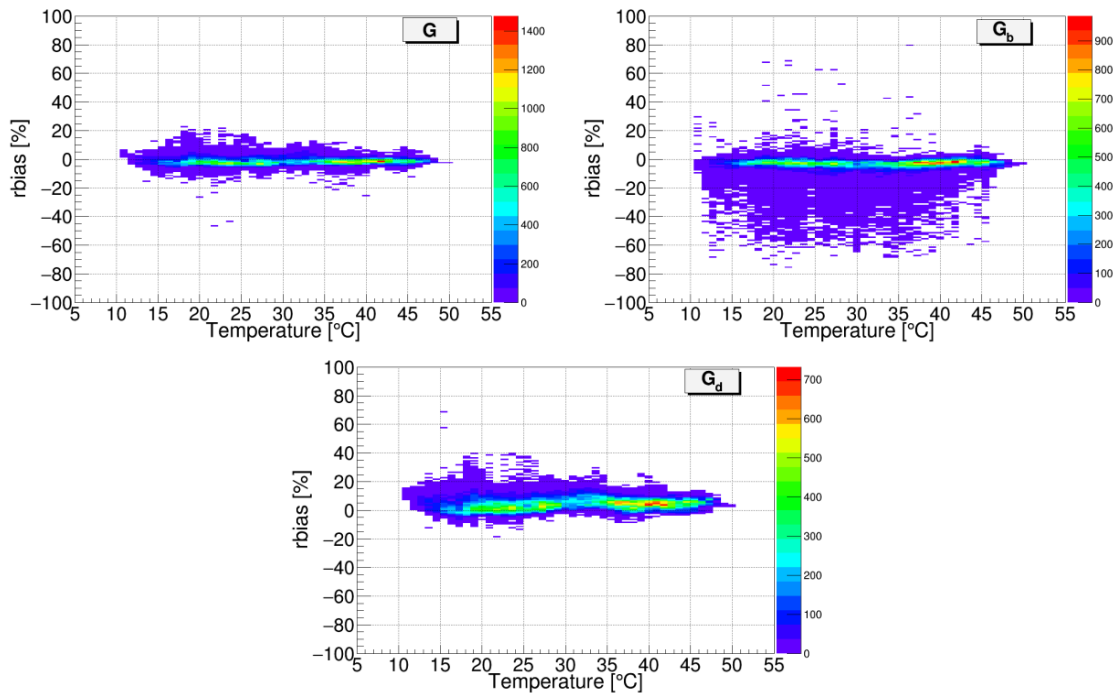


Fig.5: Relative bias of RSR vs KZ as function of air temperature for one-minute solar irradiances in Doha, Qatar.

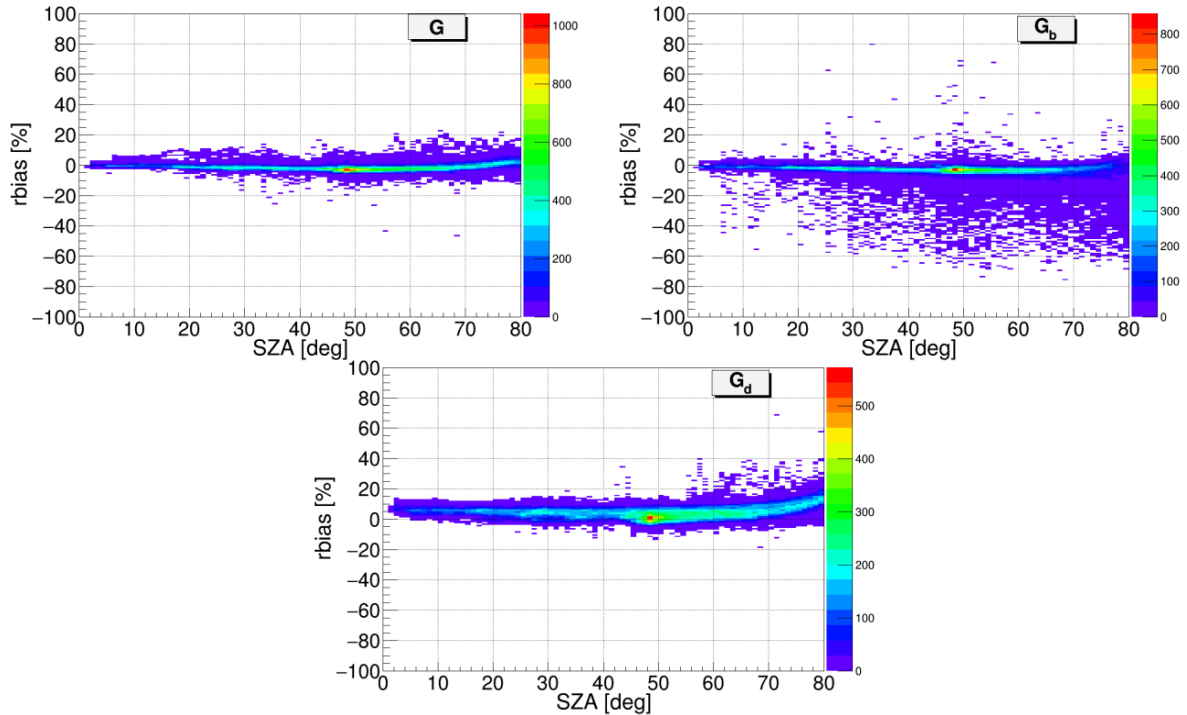


Fig.6: Relative bias of RSR vs KZ as function of sun zenith angle for one-minute solar irradiances in Doha, Qatar.

Figure 6 shows the relative bias variations with the solar zenith angle. Similarly to the previous figures, there is no clear dependency on zenith angle for the three components, and the highest deviations are observed for  $G_b$ . It was noted that there is a step in the bias of the data around SZA of  $45^\circ$  (more clearly seen in the G and  $G_d$  plots); this could be due to the moment when the direct sunlight is passing near the edges of the diffuser in the RSR, but this requires additional investigations.

#### 4. Conclusions

Ground-level measurements of solar radiation are crucial for solar resource studies as well as many other different applications. It is thus important to assess the performance, advantages and disadvantages of different measuring instruments, in order to understand the quality and uncertainties of the collected data, and evaluate their usefulness depending on the purpose and application. The study presented here shows the errors associated with measurements of solar radiation collected by an RSR device, after comparison with a higher quality solar monitoring station, under challenging desert conditions over the course of one year, in which all types of sky conditions are seen, and where aerosols produce noticeable effects on available solar radiation. The rRMSD of the RSR measurements relative to those from the thermoelectric-based station were found to be less than 3% for G, less than 4% for  $G_b$  and the highest errors were observed for  $G_d$  and were less than 6%. The corrections applied to RSR, accounting for the temperature and zenith angle effects, seem mostly correct throughout all temperature and zenith angle ranges, since no clear dependencies on ambient temperature or solar position were found; however, the correction applied to the diffuse component to account for the excess sky hidden by the shadow band seems not working correctly in all conditions seen in Qatar, in particular for those with high aerosol loads; however this needs further investigation to confirm the same.

#### 5. References

Augustyn, J., Geer, T., Stoffel, T., Kessler, R., Kern, E., Little, R., Vignola, F., Boyson, B. 2004. Update of algorithm to correct direct normal Irradiance measurements made with a rotating shadow band pyranometer. Proceedings of the American Solar Energy Society, R. Campbell-Howe and B. Wilkins-Crowder (eds.),

American Solar Energy Society, Boulder, Colorado, USA

King, M. L., Boyson, W. E., Hansen, B. R., Bower, W. I. 1998. Improved accuracy for low-cost solar irradiance sensors. World conference and exhibition of photovoltaic solar energy conversion, Vienna, Austria.

Long, C.N., Dutton, E.G., 2002. BSRN Global Network recommended QC tests, V2.0. Available online at [https://epic.awi.de/id/eprint/30083/1/BSRN\\_recommended\\_QC\\_tests\\_V2.pdf](https://epic.awi.de/id/eprint/30083/1/BSRN_recommended_QC_tests_V2.pdf). Last accessed July 2019

Pape, B., Batlles, J., Geuder, N., Piñero, R., Adan, F., Pulvermueller, B. 2009. Soiling impact and correction formulas in solar measurements for CSP projects. SolarPACES 2009, Berlin, DOI: 10.13140/2.1.4355.0406

Vignola, F. 2006. Removing systematic errors from rotating shadowband pyranometer data. In Proceedings of the American Solar Energy Society, R. Campbell-Howe, ed., American Solar Energy Society, Boulder, CO. Vignola, F., Peterson, J., Wilbert, S., Blanc, P., Geuder, N., Kern, C. 2017. New methodology for adjusting rotating shadowband irradiometer measurement. AIP Conference Proceedings, American Institute of Physics, 2017, SOLARPACES 2016, 1850 (1), pp.140021.

Wilbert, S., Geuder, N., Schwandt, M., Kraas, B., Jessen, W., Meyer, R., Nouri, B. 2015. Best practices for solar irradiance measurements with rotating shadowband irradiometers. A report of IEA SHC Task 46, Solar resources assessment and forecasting.

<http://www.irradiance.com/rsr.html>. Last accessed June 2019